Porous and Foamed Amorphous Metals

Alan H. Brothers and David C. Dunand

Abstract

This article reviews the state of the art in the field of porous amorphous metals by describing current processing techniques, mechanical properties, and potential applications. In addition to the reduction in density, the main benefit of introducing porosity in amorphous metals is the improvement in compressive ductility and energy absorption. This ductilizing effect is explained by: (1) shear-band interruption by individual pores at low porosities and (2) stable plastic bending of thin struts at higher porosities, with cellular amorphous metals displaying compressive ductilities of up to 80%.

Introduction

Of the many challenges inhibiting the use of amorphous metals in engineering applications, perhaps the most familiar and enduring is the problem of poor uniaxial ductility, which arises from the unstable propagation of shear bands.[1] The approach commonly taken to mitigate this poor ductility is interruption of those shear bands by incorporation of second phases, either precipitated during solidification or introduced through composite processing techniques.[2] Although these strategies lead to substantial improvements in compressive ductility, recent work has demonstrated that pores (which can be considered as a gaseous second phase) are equally effective in inhibiting catastrophic failures resulting from shear-band localization. In highly porous amorphous metals, propagation of shear bands can even become stable, enabling macroscopic compressive strains of more than 80% without fracture.[3]

Here, we review the state of the art in the processing of porous and foamed amorphous metals as well as current understanding in the mechanical properties of these recently developed materials. Also, we evaluate these properties within the greater contexts of amorphous metals and porous crystalline metals and propose areas for future research and applications development.

Processing

The first porous amorphous metal, made from $Pd_{43}Cu_{27}Ni_{10}P_{20}$, was described in 2003 by Schroers et al. and was produced by expansion in the liquid alloy of water vapor bubbles generated from hydrated boron oxide flux powders, followed by quenching.[4] This process, resulting in porosities of up to 85 vol% and pore sizes of ~200–1000 μm, was later modified to enable more stable bubble expansion in the low-temperature supercooled-liquid state and to create bubbles by mechanical air entrapment.[5] Also in 2003, Wada and Inoue produced open-cell structures (with fully interconnected porosity, in contrast to the closed-cell structures of the bubble expansion method) with 65 vol% of 125–250 μm pores, by casting $Pd_{42.5}Cu_{30}Ni_{7.5}P_{20}$ into beds of NaCl particles, quenching, and removing the salt by dissolution.[6] Beginning in 2004, Wada and Inoue also foamed this alloy by the expansion of hydrogen bubbles precipitated from a supersaturated melt, yielding porosities of up to 71% with pore sizes of 80 μm and smaller.[7–10] Inoue et al. later applied the method to a slightly different composition, $Pd_{35}Pt_{15}Cu_{30}P_{20}$.[11] These foams illustrate processing methods suitable for very stable, noble-metal alloys.

Brothers and Dunand reported in 2004 the first amorphous foam using a commercial alloy, $Zr_{57}Nb_5Cu_{15.4}Ni_{12.6}Al_{10}$ (Vit106), which was produced by melt infiltration of beds of hollow carbon microspheres with diameters of 25–50 μm.[12] Beginning in 2005, Brothers et al. demonstrated the use of the replication method for amorphous foams, in which liquid Vit106 was infiltrated into a packed bed of BaF_2 salt particles that was removed after solidification in an acid bath. With this method, porosities in the range of 72–86% were demonstrated, with pore sizes in the range of 150–350 μm.[13–16] In 2006, a similar foam with lower porosity (36–41%) and larger pore size (approximately 500–1000 μm) was produced by Ren and Qiu from $Zr_{41.25}Ti_{13.75}Cu_{12.5}Ni_{10}Be_{22.5}$ using NaCl placeholders.[17,18] Images of several representative porous amorphous metals, produced using liquid-state methods, are shown in Figure 1. These methods demonstrated the possibility of foaming reactive Zr-based alloys of the sort used in most metallic glass applications.

Also in 2006, Jayaraj et al.[19] reported successful processing of nanoporous Ti-based amorphous metal ribbons using a method proposed in 2004 by Gebert et al. for a La-based metallic glass,[20] in which one phase is selectively acid-leached from a two-phase amorphous metal. Ribbons produced in this manner by Jayaraj et al. contained fully interconnected porosity, with the finest pore sizes reported in any amorphous metal to date (15–155 nm), and thus represent the first nanoporous amorphous metals.

A similar method was concurrently developed by Lee and Sordelet,[21,22] where the sacrificial phase is crystalline rather than amorphous, and the starting two-phase material is formed by warm extrusion of powder blends rather than casting. The authors demonstrated their method by producing porous $Cu_{47}Ti_{33}Zr_{11}Ni_8Si_1$ (porosity 32%, pore sizes from <0.1 μm to ~2 μm) through selective dissolution of crystalline Cu,[21] as well as porous $Ni_{59}Zr_{20}Ti_{16}Si_2Sn_3$ (porosity, 40%; average pore size, 10–50 μm) by dissolution of bronze.[22] The resulting materials are distinguished from those of Jayaraj et al.[19] by their highly elongated pore structures, which result from extrusion of the powders before the acid treatment.

These dissolution processes are notable by virtue of being performed in the solid state, whereas the previous foaming methods involved the liquid and supercooled-liquid states. Two other powder-based methods were reported in 2006. Xie et al. reported amorphous $Zr_{55}Cu_{30}Al_{10}Ni_5$ with up to 67% porosity produced by partial spark-plasma consolidation of amorphous powders with diameters of 37–53 μm.[23] Hasegawa et al. also studied the effects of lower levels (approximately 2%) of porosity retained in melt-spun ribbons of the same alloy, prepared from powder compacts containing aluminum nitride.[24] Representative powder-processed porous amorphous metals are shown in Figure 2.

The above review, which spans the 2003–2006 time range, illustrates the rapid

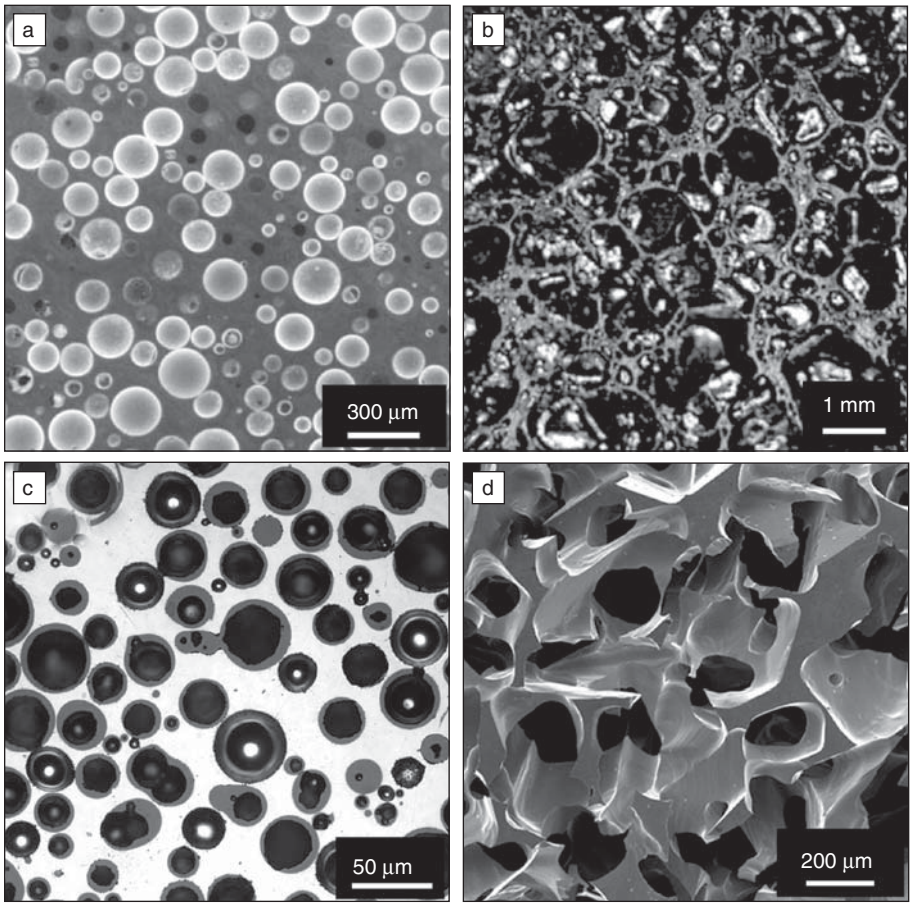

Figure 1. Examples of amorphous metal foams created by liquid-state and supercooled-liquid-state methods. (a) Pd-based foam (porosity P = 42–46%) made by precipitation of dissolved hydrogen gas during cooling.[7] (b) Pd-based foam (P = 85%) made by entrapping gas in the melt and then expanding it in the supercooled-liquid state.[5] (c) Zr-based foam made by infiltration of a bed of hollow carbon spheres. Volume fraction of spheres in the foam is 59%.[12] (d) Zr-based foam (P = 78%) made by infiltration of BaF_2 salt particles followed by removal of those particles in an acid bath.[14]

advances made in creating porous amorphous metals. Methods now exist for producing foams from various amorphous alloys (Ti-, Ni-, Cu, Zr-, Pd-, and La-based), with both isolated and fully interconnected pore structures consisting of spherical or angular pores with equiaxed or elongated shapes. Pore sizes ranging from the submicrometer to the millimeter scale and porosities ranging from 2% to more than 85% have been reported. Alternative processing methods, used for crystalline metal foams but not yet demonstrated for amorphous metals, are described in a recent review article.[3] It is hoped that such alternative processes will reduce cost and complexity by eliminating expensive or hazardous steps such as leaching in concentrated strong acids and high-temperature, high-pressure hydrogen gas charging.

Mechanical Properties

As suggested in the Introduction, the primary purpose of introducing porosity in amorphous metals is to hinder the propagation of shear bands. Two main mechanisms of hindering shear-band propagation have been identified: shear-band disruption and shear-band stabilization.

Shear-band disruption relies on the same mechanisms active in amorphous metal-matrix composites. Pores (like solid inclusions) interrupt shear bands when their paths intersect, favoring branching of those bands and/or nucleation of new bands. Pores also perturb the local stress fields in the surrounding matrix and thereby deflect shear bands (increasing their path length, and hence the energy they dissipate) or even arrest them by diminishing the local stresses that drive their motion.[2,8] Unlike solid inclusions, however, pores can also act as blunt cracks; in amorphous metals, large crack-tip radii favor multiple shear banding and are attended by increases in toughness that are abnormally large relative to crystalline metals.[2]

Although these effects can explain the large compressive ductility (on the order of 25%) observed even in low-porosity (<4%) systems,[8,10,11] it is notable that the largest compressive ductility, upwards of 80% strain, was reported in amorphous cellular metals (i.e., foams with porosity exceeding ~40%).[9,14] These materials are best viewed as interconnected networks of amorphous metal struts, rather than contiguous matrices containing distinct pores. Such an architecture enables them to benefit from a ductilizing mechanism known as shear-band stabilization,[25–27] first noted during bending of thin amorphous metal wires and foils.

The shear bands developed within bending wires and foils become more shallow as the wire or foil thickness decreases, with two results. First, each band relaxes the stress from a smaller volume of the surrounding glass, enabling a closer spacing of the neighboring shear bands subsequently initiated, thereby increasing band density and overall plastic strain. Second, shallower shear bands produce smaller shear offsets at the surfaces of the wires or foils, and these smaller offsets reduce the probability of nucleating a crack. In the case of Zr-based alloys, shear-band stabilization becomes noticeable for wire or foil thicknesses below about 1 mm.[25]

Just as for individual wires and foils, the slender, randomly oriented struts within foam materials deform primarily in bending, even during uniaxial compression of the foam,[28] and thus can benefit from shear-band stabilization. The effectiveness of shear-band stabilization in ductilizing amorphous metal foams is made clear by the large compressive strains (>80%, well beyond the ductility observed in amorphous composites, which is typically <30%) measured in those materials.[14]

To illustrate the effectiveness of porosity in improving ductility and energy absorption in amorphous metals, several compressive stress–strain curves for porous amorphous metals with porosities between 3.7% and 82% are shown in Figure 3.[7–9,13] For comparison, the stress–strain behavior of dense $Pd_{42.5}Cu_{30}Ni_{7.5}P_{20}$ (which is the base alloy for most of the curves in the figure) is also shown.[7] With increased porosity, the amorphous samples show decreasing strength and stiffness, along with drastically increasing ductility and progressively "flatter"

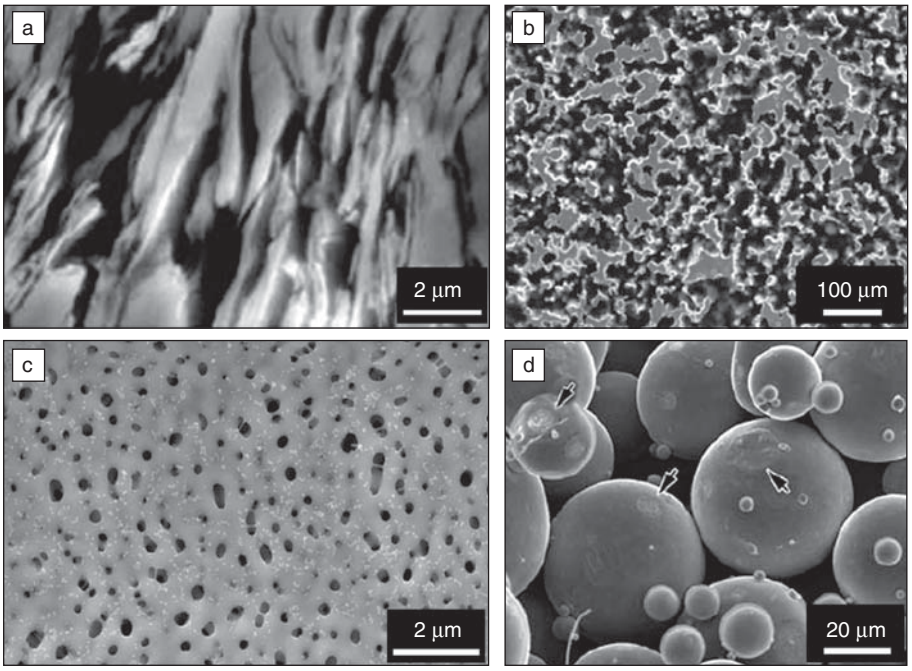

Figure 2. Examples of powder-processed porous amorphous metals and amorphous metal foams created by solid-state methods. (a) Cu-based foam (porosity $P = 75\%$) made by dissolution of crystalline Cu from an extruded composite.[21] (b) Ni-based foam ($P = 42\%$) made by dissolution of brass from an extruded composite.[22] (c) Ti-based porous amorphous metal (P not given) made by selective dissolution of one phase from a two-phase amorphous metal.[19] (d) Zr-based porous compact ($P = 34\%$) made by partial electroconsolidation of amorphous powders.[23]

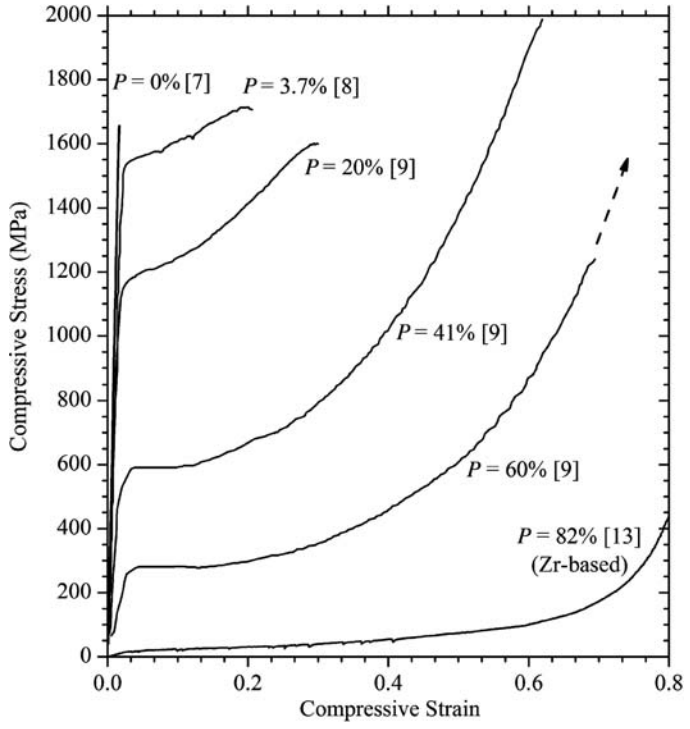

Figure 3. Compressive engineering stress–strain curves for several porous amorphous metals at intervals of approximately 20% porosity P. All but the highest-porosity material (which was processed from $Zr_{57}Nb_5Cu_{15.4}Ni_{12.6}Al_{10}$) were processed from $Pd_{42.5}Cu_{30}Ni_{7.5}P_{20}$.

stress–strain behavior. Most notable are the extremes of behavior shown in the figure: a large ductilizing effect is already visible at very low porosities near 4%, where strength and stiffness are only minimally affected, whereas at the highest porosities, compressive ductility becomes comparable to that of foam materials made from highly ductile crystalline metals such as aluminum.[28]

A more comprehensive illustration of compressive ductility in porous amorphous metals is shown in Figure 4, where failure strains are compiled as a function of porosity. Despite a few outliers, the data indicate two types of behavior: as highlighted by the upper dashed line, most porous amorphous metals gain substantial compressive ductility (approximately 10–80% failure strain), even from low levels of porosity; yet as shown by the lower dashed line, some structures lead to almost no ductilization (approximately 2–4% failure strain), even at relatively high porosities. Thus, it is not only the porosity fraction, but also pore morphology and distribution that determine the effectiveness of the ductilizing mechanisms described above. The strongest illustration of this point was provided by Wada et al.,[9] who showed that for Pd-based amorphous foams with the same overall porosities of 3% and 11%, elliptical pores with long axes parallel to the loading axis induce little or no plasticity (markers with vertical strikethroughs in Figure 4), whereas pores with long axes perpendicular to the loading axis result in up to 20–30% compressive strain to failure (open square symbols with horizontal strikethroughs in Figure 4). It is also important to note that in keeping with the behavior of porous crystalline metals, pores in amorphous metals do not improve ductility in tension, but rather act as cracks.[8]

Available data for the compressive yield strength and loading stiffness of porous amorphous metals are compiled in Figure 5 (as for Figure 4, only data provided explicitly in published reports are included in the figure). As shown in Figure 5a, porous amorphous metals span a wide range of strengths, from less than 10 MPa for high-porosity foams to nearly 2 GPa for near-dense alloys. As shown in previous reviews,[3,11] the foam relative strength and stiffness (i.e., normalized by strength and stiffness of the solid material) can be fitted well over a range of relative porosities to power-law equations that are valid for cellular crystalline metals.[28]

Applications

The available mechanical property data for amorphous metals (Figures 3–5)

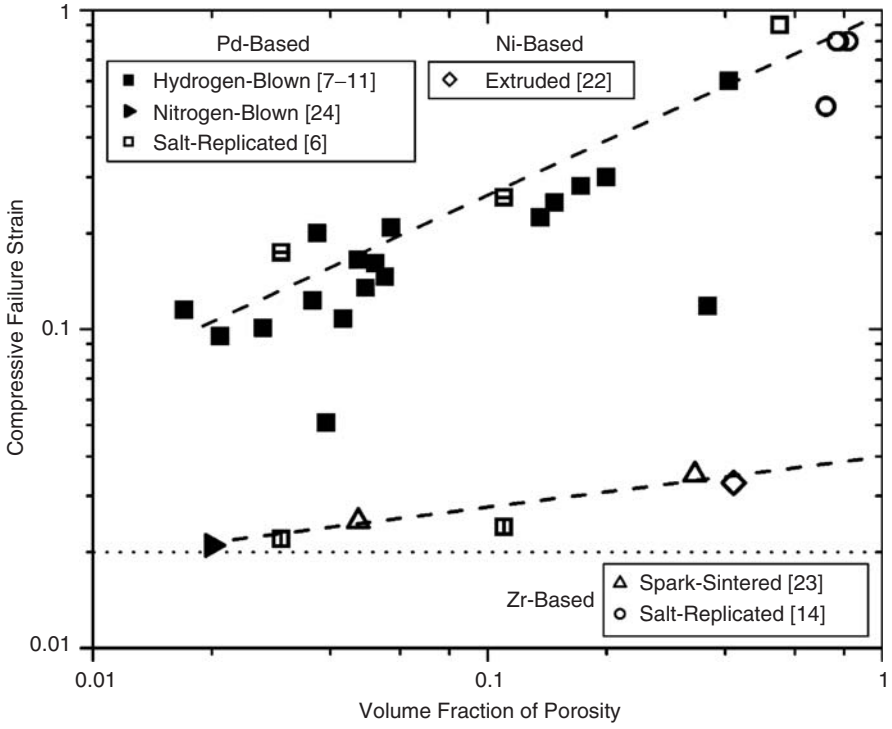

Figure 4. Compressive strain to failure as a function of porosity for published porous amorphous metals. Composition and processing methods are summarized in the labels. Open and solid symbols represent open-cell and closed-cell structures, respectively. Open squares with strikethroughs represent materials with elliptical porosity oriented parallel (vertical strikethroughs) and perpendicular (horizontal strikethroughs) to the loading axis.[9] The horizontal line at a failure strain of 2% is representative of fully dense amorphous metals.[1] The dashed lines are visual aids used to demonstrate how certain structures (upper line) produce substantial ductility, while others (lower line) produce less ductility.

suggest that porosity can be used as a means of modifying the properties of amorphous metals smoothly between those of monolithic alloys (high strength and stiffness with low ductility and high density) and those of crystalline metal foams (low strength and stiffness with very large compressive ductility and low density), that is, as a means of selectively and continuously trading strength and stiffness for ductility, weight reduction, and energy absorption. As a result, porous amorphous metals could find use in a variety of applications, from structural materials (where high strength and modest ductility are required) to energy-absorption or packaging applications (where low load transfer, i.e., low flow stresses, are needed in combination with large compressive failure strain to maximize energy absorption).

The application of porous amorphous metals as high-strength structural materials appears realistic in compressive applications (from a properties standpoint, if not yet an economic one) because, as illustrated in Figures 3–5, low porosity levels induce substantial compressive plasticity (approximately 20%) with only small relative losses in strength (less than about 10%),[8,10] because at low porosities the ductilizing effect outpaces the weakening effect. At larger porosities, amorphous metals show compressive ductility on par with foams made from ductile crystalline metals and may therefore compete in

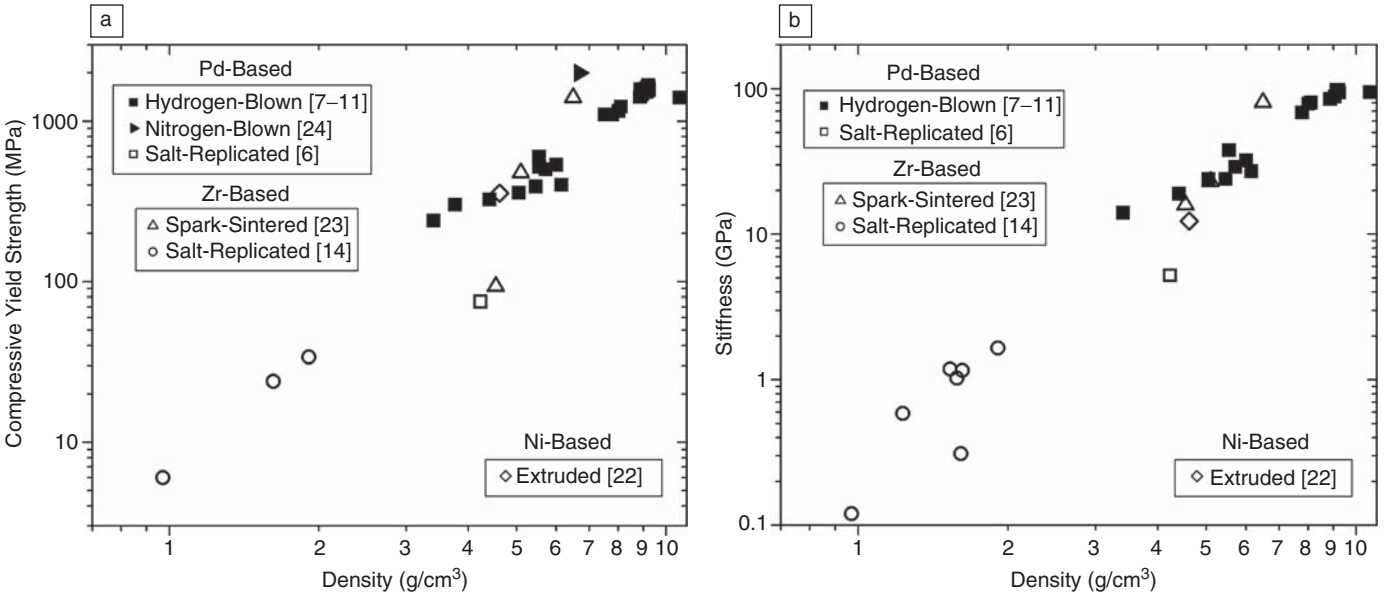

Figure 5. (a), (b) Compressive yield strength and stiffness as functions of density for published porous amorphous metals. Composition and processing methods are summarized in the labels. Open and solid symbols represent open-cell and closed-cell structures, respectively. Densities of the pore-free Zr-, Ni- and Pd-based glasses are 6.8 g/cm^3, 7.9 g/cm^3, and 9.4 g/cm^3, respectively.

applications for which crystalline metallic foams are currently used (e.g., lightweight structural members and energy absorbers).[28] Low-density amorphous Zr-based foams already show better energy absorption capacity, when compared on a volumetric basis, than crystalline aluminum-based foams, and their higher strength could make them useful in the protection of sturdier foam-core components for vehicles.[14]

In terms of energy absorption per unit mass, however, it is unclear whether this advantage persists. The large difference in solid density between Zr-based glasses and crystalline Al alloys implies that foams of equal absolute density will have very different pore fractions and, hence, qualitatively different compressive behavior. For instance, a foam density of 1 g/cm^3 represents ~15% relative density for a Zr-based amorphous foam, but 37% relative density for an Al foam; it is difficult to fairly compare energy absorption between such foams, as their stress–strain curves will differ in shape. Making full use of the high specific strength of amorphous metals for structural applications may therefore require the use of light-metal amorphous foams rather than the heavier amorphous alloys used in foaming studies to date. Much has already been achieved in the development of Mg-based bulk metallic glasses,[29] but strong glass-formers based on Al still prove elusive.[30]

In all such applications, porous amorphous metals would also enjoy the intrinsic benefits of amorphous metals, such as large elastic energy return, wear resistance, and, in certain cases, corrosion resistance and unique magnetic properties.[1] Such properties might also recommend open-cell amorphous metals for multifunctional applications such as fluid filters or bone replacement. The latter of these seems particularly promising, given the demonstrated capacity for producing open-cell amorphous Zr-based foams with good corrosion resistance and strength, but low stiffness (aided by the low characteristic elastic moduli of amorphous metals[1]) that can be designed to match that of natural bone. However, important limitations remain, such as low tensile ductility, cooling rate limitations, and high costs (associated with expensive high-purity alloy components, to which must be added the cost of the foaming process). Also unknown at present are key mechanical properties of amorphous foams, such as resistance to fatigue and tensile fracture.

Conclusions

Porous amorphous metals represent a promising new step toward the engineering application of amorphous metals by enabling mechanical properties and density to be varied across a wider range than is possible using monolithic alloys or composites. By controlling levels of porosity, compressive strength and stiffness can be varied from near-maximum values (e.g., for structural components) to almost arbitrarily low values (e.g., for energy absorption applications), whereas compressive failure strains can be varied from ~2% to more than 80%. Porosity introduction can optimize density-compensated mechanical properties and tailor other properties such as fluid permeability, specific surface area, and acoustic damping to meet the requirements of applications such as load-bearing components, crash and impact mitigators, filters or electrode materials, and biomedical implants.

References

1. A.R. Yavari, J.J. Lewandowski, J. Eckert, *MRS Bull.* **32** (8) (2007) p. 635.
2. J.J. Lewandowski, M. Shazly, A.S. Nouri, *Scripta Mater.* **54**, 337 (2006).
3. A.H. Brothers, D.C. Dunand, *Scripta Mater.* **54**, 513 (2006).
4. J. Schroers, C. Veazey, W.L. Johnson, *Appl. Phys. Lett.* **82**, 370 (2003).
5. J. Schroers, C. Veazey, M.D. Demetriou, W.L. Johnson, *J. Appl. Phys.* **96**, 7723 (2004).
6. T. Wada, A. Inoue, *Mater. Trans.* **44**, 2228 (2003).
7. T. Wada, A. Inoue, *Mater. Trans.* **45**, 2761 (2004).
8. T. Wada, A. Inoue, A.L. Greer, *Appl. Phys. Lett.* **86**, 251907 (2005).
9. T. Wada, M. Kinaka, A. Inoue, *J. Mater. Res.* **21**, 1041 (2006).
10. T. Wada, K. Takenaka, N. Nishiyama, A. Inoue, *Mater. Trans.* **46**, 2777 (2005).
11. A. Inoue, T. Wada, X.M. Wang, A.L. Greer, *Mater. Sci. Eng.* **A442**, 233 (2006).
12. A.H. Brothers, D.C. Dunand, *Appl. Phys. Lett.* **84**, 1108 (2004).
13. A.H. Brothers, D.C. Dunand, *Adv. Mater.* **17**, 484 (2005).
14. A.H. Brothers, D.C. Dunand, *Acta Mater.* **53**, 4427 (2005).
15. A.H. Brothers, D.W. Prine, D.C. Dunand, *Intermetallics* **14**, 857 (2006).
16. A.H. Brothers, R. Scheunemann, J.D. DeFouw, D.C. Dunand, *Scripta Mater.* **52**, 335 (2005).
17. K.Q. Qiu, Y.L. Ren, *J. Mater. Sci. Technol.* **21**, 788 (2005).
18. Y.L. Ren, Z.Y. Suo, K.Q. Qiu, *Acta Metall. Sinica* **42**, 379 (2006).
19. J. Jayaraj, B.J. Park, D.H. Kim, W.T. Kim, E. Fleury, *Scripta Mater.* **55**, 1063 (2006).
20. A. Gebert, A.A. Kundig, L. Schultz, K. Hono, *Scripta Mater.* **51**, 961 (2004).
21. M.H. Lee, D.J. Sordelet, *Scripta Mater.* **55**, 947 (2006).
22. M.H. Lee, D.J. Sordelet, *Appl. Phys. Lett.* **89**, 021921 (2006).
23. G. Xie, W. Zhang, D. Louzguine-Luzgin, H. Kimura, A. Inoue, *Scripta Mater.* **55**, 687 (2006).
24. M. Hasegawa, D. Nagata, T. Wada, A. Inoue, *Acta Mater.* **54**, 3221 (2006).
25. R.D. Conner, W.L. Johnson, N.E. Paton, W.D. Nix, *J. Appl. Phys.* **94**, 904 (2003).
26. R.D. Conner, Y. Li, W.D. Nix, W.L. Johnson, *Acta Mater.* **52**, 2429 (2004).
27. G. Ravichandran, A. Molinari, *Acta Mater.* **53**, 4087 (2005).
28. M.F. Ashby, T. Evans, N.A. Fleck, L.J. Gibson, J.W. Hutchinson, H.N.G. Wadley, *Metal Foams: A Design Guide* (Butterworth-Heinemann, Boston, 2000).
29. H. Ma, L.L. Shi, J. Xu, Y. Li, E. Ma, *Appl. Phys. Lett.* **87**, 181915 (2005).
30. R.D. Sa Lisboa, C. Bolfarini, W.J.F. Botta, C.S. Kiminami, *Appl. Phys. Lett.* **86**, 211904 (2005). □